Journal of Aerosol Science 79 (2015) 1–14

Contents lists available at ScienceDirect

Journal of Aerosol Science

journal homepage: www.elsevier.com/locate/jaerosci

Offline thermal-desorption proton-transfer-reaction mass spectrometry to study composition of organic aerosol

J. Timkovsky [a,*], U. Dusek [a,c], J.S. Henzing [b], T.L. Kuipers [a], T. Röckmann [a], R. Holzinger [a]

[a] Institute for Marine and Atmospheric Research Utrecht, Utrecht University, PO box 80005, 3508 TA, the Netherlands
[b] Netherlands Organisation for Applied Scientific Research (TNO), Utrecht, the Netherlands
[c] University of Groningen, the Netherlands

ARTICLE INFO

Article history:
Received 9 May 2014
Received in revised form
28 August 2014
Accepted 29 August 2014
Available online 10 September 2014

Keywords:
Organic aerosol
Composition
Measurements
Artifacts

ABSTRACT

We present a novel approach to study the organic composition of aerosol filter samples using thermal-desorption proton-transfer-reaction mass spectrometry (TD-PTR-MS) in the laboratory. The method is tested and validated based on the comparison with in situ TD-PTR-MS measurements. In general, we observe correspondence within the levels of uncertainty between in situ and offline TD-PTR-MS measurements for compounds desorbing at temperatures above 100 °C and for quartz fiber filters that were sampled for more than one day. Positive sampling artifacts (50–80%, with respect to the in situ measurements) from adsorption of semivolatile organic gas phase compounds are apparent on filters sampled for one day. Detailed chemical analysis shows that these positive sampling artifacts are likely caused by primary emissions that have not been strongly oxidized. Negative sampling artifacts (7–35%, with respect to the in situ measurements) are observed for most filters sampled for two and three days, and potentially caused by incomplete desorption of aerosols (in particular, nitrogen-containing organics) from the filters during the offline measurements and chemical reactions on the filters.

© 2014 Elsevier Ltd. All rights reserved.

1. Introduction

Atmospheric aerosols have been studied intensively because of their impact on climate and their health effects. Organic aerosol (OA) typically accounts for 20–90% of the total aerosol mass (Kanakidou et al., 2005). The chemical composition of organic aerosol is very complex and has not been resolved completely at a molecular level. It has been characterized using a suite of online and in situ instruments in field studies: for example, aerosol mass spectrometer (AMS) (e.g., Jayne et al., 2000), micro-orifice volatilization impactor coupled to a chemical ionization mass spectrometer (MOVI–CIMS) (e.g., Yatavelli & Thornton, 2010), particle-into-liquid sampler (PILS) (e.g., Weber et al., 2001), filter inlet for gases and aerosols (FIGAERO) (Lopez-Hilfiker et al., 2014), in situ thermal-desorption proton-transfer-reaction mass spectrometer (TD-PTR-MS) (e.g., Holzinger et al., 2010a) and thermal desorption aerosol gas chromatograph/mass spectrometer (TAG) (Williams et al., 2006). These in situ methods are powerful tools

* Corresponding author.
E-mail address: j.timkovsky@uu.nl (J. Timkovsky).

http://dx.doi.org/10.1016/j.jaerosci.2014.08.010
0021-8502/© 2014 Elsevier Ltd. All rights reserved.

to get information on aerosol composition, but field studies using these instruments are expensive and often can cover only limited time periods.

In order to be able to perform long-term aerosol measurements at low cost, sampling of aerosol on filters with offline analysis in the laboratory is often used (e.g., ten Brink et al., 2004; Subramanian et al., 2004; Viana et al., 2006, 2007). Among the advantages of offline methods are easy implementation of sampling and the possibility to sample a large volume of air, which allows for a low detection limit. Furthermore, filter samples can be stored and measured with offline methods later, whereas online aerosol composition data cannot be obtained or re-measured after a field campaign is over. Among the disadvantages of organic aerosol sampling on filters are complicated sampling artifacts. Two principal types of artifacts have been observed: positive (i.e. the aerosol concentrations determined based on the offline technique are overestimated) and negative (the corresponding concentrations are underestimated).

Positive artifacts can be caused by the adsorption of organic vapors on the filters and are difficult to quantify (Turpin et al., 2000), because they depend on sampling time, location and face velocity (McDow & Hunzicker, 1990; Turpin et al. 1994; Subramanian et al., 2004). Moreover, it was shown that filters manufactured by the same company, but having different lot number, exhibit different organic vapor adsorption capacity (Kirchstetter et al., 2001). Negative artifacts are caused by volatilization of compounds that have been already collected on filters, e.g. relatively light polycyclic aromatic hydrocarbons (PAHs) (Coutant et al., 1988). Additionally, Schauer et al. (2003) showed that chemical reactions on the filters can cause a negative artifact for measurements of particle-bound PAHs in the atmosphere (up to 100% underestimation).

Both negative and positive artifacts are particularly influenced by semivolatile organic compounds (SVOCs), which partition between the gas and the condensed phases. Lipsky and Robinson (2006) showed that the degree of dilution strongly influences the partitioning of SVOCs in diesel exhaust. They discovered that SVOCs tend to be in the gas phase when the exhaust is diluted (causing negative artifacts on filter samples), and the SVOCs tend to be in the condensed phase when exhaust is undiluted (causing positive artifacts). Some attempts have been made to quantify the partitioning of SVOCs, but it is problematic to apply this quantification to real-atmosphere conditions (e.g., Mader & Pankow, 2001).

Attempts to correct for the artifacts using field blanks, backup filters and denuders have been performed. Nevertheless, the filter material itself influences the magnitude of sampling artifacts (Turpin et al., 2000). In general, quartz fiber filters are used for aerosol sampling due to their high temperature resistance. The latter is needed for organic carbon measurements, which require high temperatures for complete desorption. However, high positive artifacts are observed for the quartz filters due to their high specific area and consequently high gas adsorption. As an alternative, the use of Teflon filters is possible with lower specific area. On the other hand, these filters cannot withstand high temperatures needed to desorb most of OA (Turpin et al., 2000). The use of a quartz backup filter along with a quartz front filter is common. However, e.g., Watson et al. (2009) discovered in an extensive study that the use of backup filters (and field blanks) does not fully represent filter sampling artifacts. Viana et al. (2006) showed that the use of a diffusion denuder might reduce organic carbon (OC) mass observed without a denuder by 34%, therefore correcting for positive artifacts. However, they also found that the use of such a denuder does not provide a good comparability between high- and low-volume filter samplers.

While multiple studies have been performed to examine total organic carbon artifacts, there is only a limited number of investigations where artifacts are studied along with the chemical composition of OA. For example, Lambe et al. (2010) performed more detailed studies on the chemical composition of organic aerosols sampled on filters. They compared GC–MS analysis of organic aerosol desorbed from filter samples to in situ TAG measurements for a limited set of compounds (n-alkanes, PAHs, and hopanes). Based on the ambient air measurements they found reasonable agreement for hopanes (r^2=0.55–0.95, slope=1.0–1.7) and PAHs (r^2=0.58–0.97, slope=0.8–1.0). However, for n-alkanes (C27–C32) the agreement was poor: r^2=0.17–0.85, slope=0.4–1.7, and the exact reason for this was not established.

The objectives of this study were (i) to introduce and validate a new offline analytical technique based on quartz fiber filter sampling and subsequent analysis by thermal-desorption proton-transfer-reaction mass-spectrometry (TD-PTR-MS) and (ii) to use this method to investigate some filter sampling artifacts in more detail. We evaluate and characterize the new offline method by comparison with in situ TD-PTR-MS measurements (Holzinger et al., 2010a). The in situ TD-PTR-MS measurements and filter sampling were performed at the same time and location and in both analyses the same instrument (PTR-TOF-MS) was used, facilitating direct comparison of the two datasets.

2. Experimental methods

2.1. Measurement campaign

The measurement campaign for comparison of the in situ TD-PTR-MS, the filter-based TD-PTR-MS (referred to as 'offline' method hereafter) and the Scanning Mobility Particle Sizer (SPMS) methods took place from 8 February 2011 till 7 March 2011 at the Cabauw Experimental Site for Atmospheric Research (CESAR)[1] about 20 km south-west of the city of Utrecht in the Netherlands (51.971°N, 4.927°E). The inlet for the in situ measurements was located at the height of ~5 m above the ground and a high volume filter sampler was located directly on the ground and sampled 2 m above the ground at a distance of ~4 m from the TD-PTR-MS inlet. The inlet of the SMPS was located at 60 m height on the Cabauw tall tower.

[1] http://www.cesar-observatory.nl/

Table 1
Time periods during which the filters were located in the field. All filters, except for field blanks, are in bold and the respective sampling time periods are shown. The number of replicas per filter measured in the laboratory is shown. In case the main wind direction changed during sampling, 'A' corresponds to the first half of the sampling and 'B' – to the second half.

Filter#	Sampling period	Sampling duration (h)	# of replicas	Wind direction	Ambient air conditions
CA3	11 February 2011 ~ 14:00–17 February 2011 ~ 14:00	0	3		
CA5	**15 February 2011 14:00–16 February 2011 14:00**	**24**	**3**	**South westerly**	**Normal**
CA6	**16 February 2011 14:00–17 February 2011 14:00**	**24**	**3**	**South easterly**	**Normal**
CA10	**23 February 2011 13:15–25 February 2011 13:15**	**48**	**3**	**A.Westerly; B.Southerly**	**Normal**
CA11	**25 February 2011 13:15–27 February 2011 13:15**	**48**	**3**	**A. North westerly; B. South westerly**	**Mixed**
CA12	**27 February 2011 14:15–1 March 2011 14:15**	**48**	**3**	**Easterly**	**Polluted**
CA13	**1 March 2011 13:15–4 March 2011 13:15**	**72**	**1**	**Easterly**	**Polluted**
CA14	1 March 2011 ~ 13:00–4 March 2011 ~ 13:00	0	2		
CA15	**4 March 2011 14:52–7 March 2011 14:52**	**72**	**3**	**Northerly**	**Mixed**

During the campaign 7 filters (CA5, CA6, CA10–CA13, CA15) and two field blanks (CA3 and CA14) were collected. The sampling times for the filters are shown in Table 1. The air mass history of the various air samples was evaluated by calculating 72 h back trajectories using the model HYSPLIT (Draxler & Rolph, 2013; Rolph, 2013). During the campaign different synoptic conditions were encountered, which are generally characterized by the wind directions, which are indicated in Table 1. The offline measurements were performed in the laboratory within one month after the field campaign (end of March, 2011).

2.2. Instrument description

The measurements were performed using a standard PTR-TOF8000 instrument (Ionicon Analytik GmbH, Austria, from here on referred to as 'PTR-MS'), which has been described previously (Jordan et al., 2009; Graus et al., 2010). In short, this instrument allows for precise measurements of volatile organic compounds (VOCs) in air or nitrogen. The soft chemical ionization using H_3O^+ ions to protonate the VOCs is a proven technique of ionization with limited fragmentation. The time-of-flight mass spectrometer allows for a high mass resolution ($m/\Delta m \sim 4000$). Therefore, ions with differences in m/z bigger than ~30 mDa (depending on the mass value) can be distinguished (e.g., m/z 69.034 and m/z 69.070) and corresponding empirical formulas ($C_4H_5O^+$ and $C_5H_9^+$, respectively) can be attributed. The recorded mass spectra covered a mass range 15–1157 Da. 83340 individual mass spectra were averaged over time to obtain a time resolution of 5 s.

The general settings of the PTR-MS instrument were equal for both setups: drift tube temperature, 120 °C, inlet tube temperature, 180 °C, drift tube pressure, 2.3–2.5 hPa; ion source voltages, $U_s = 120–140$ V, $U_{so} = 92$ V; E/N, 125–127 Td; extraction voltage at the end of the drift tube, $U_{dx} = 24$ V. The ion source current was kept between 4 and 5 mA and a water flow of 3.5–4 mL/min (unless otherwise stated volume flow rates refer to standard conditions: 1013.25 hPa, 273.15 K) was provided to the ion source. The intensity of the primary H_3O^+ ion signal (detected at m/z 21.023) during all PTR-MS measurements was higher than 2.5×10^5counts per second (cps) which ensured sensitivities of order of 10 cps/ppb.

2.2.1. The in situ TD-PTR-MS method

The in situ TD-PTR-MS setup consists of an aerosol inlet system coupled to the PTR-MS (Fig. 1A). It has been described in detail previously (Holzinger et al., 2010a). Briefly, ambient air was sampled through the copper inlet with a PM2.5 pre-cutoff. The sampled air passed through a humidifier and the particles were collected on the Collection-Thermal-Desorption (CTD) cell. The CTD cell is specified to sample particles in the size range 0.07–2 μm at relative humidity levels above 70% (Holzinger et al., 2010a). With respect to filter sampling the collection efficiency of in situ TD-PTR-MS is lower and therefore we expect that concentrations measured with the in situ technique are also lower (depending on the actual size distribution this may be 10–20%, but rarely above 30%). After collection, the particles were desorbed by heating up the CTD cell in steps of 50 °C for a duration of 3 min, starting at 50 °C and going up to 350 °C. A flow of nitrogen (ultrapure nitrogen, 5.7 purity, Air Products) transferred the desorbed species to the PTR-MS. As a result a thermogram was obtained, defined as a measured ion signal intensity profile over a range of temperatures.

The system was equipped with two identical aerosol inlets (A and B). This setup allowed aerosol sampling with one inlet while analyzing the aerosols collected with the second inlet. The collection time for both inlets was 30 min. The whole in situ TD-PTR-MS measurement cycle is shown in Fig. 2, m/z 85.028 is used as an example. The instrument background was measured by passing ambient air through a Teflon membrane filter (Zefluor 2.0 μm, Pall Corp.) located in the system (one filter per inlet). The filters were changed once per week during the campaign. Background measurements were performed once per three measurements (Fig. 2). In a thermogram measurement we observed signals corresponding to the compounds that are

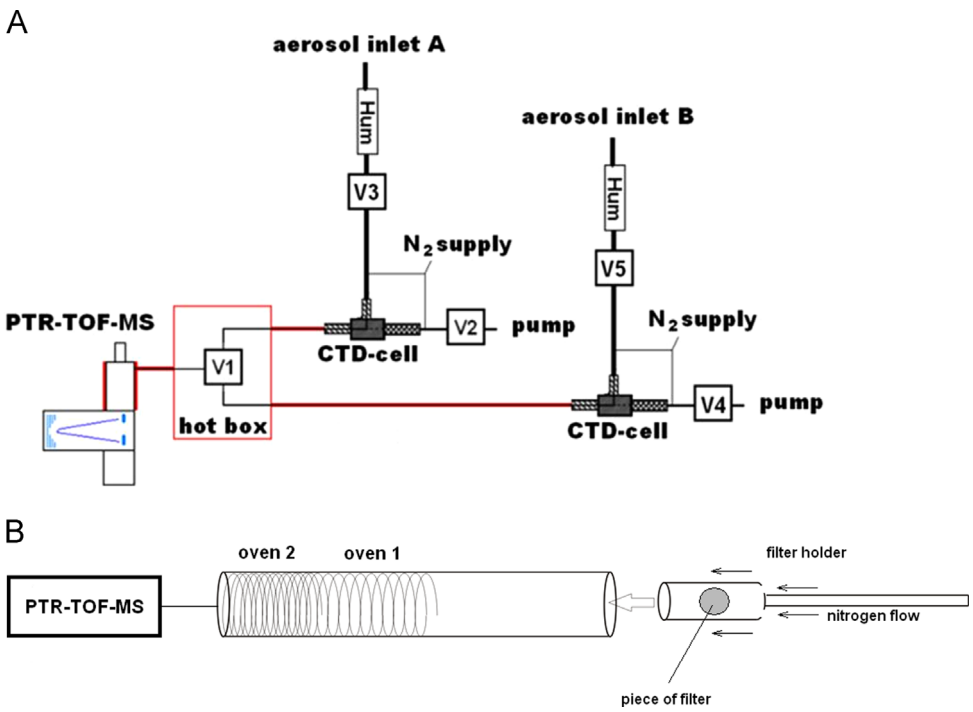

Fig. 1. The in situ (A) and offline (B) TD-PTR-MS setups. The following valves are present on scheme A: V1 – allows switching between two aerosol inlets, and V2–V5 – allow switching between sampling and measuring modes for inlet A and B.

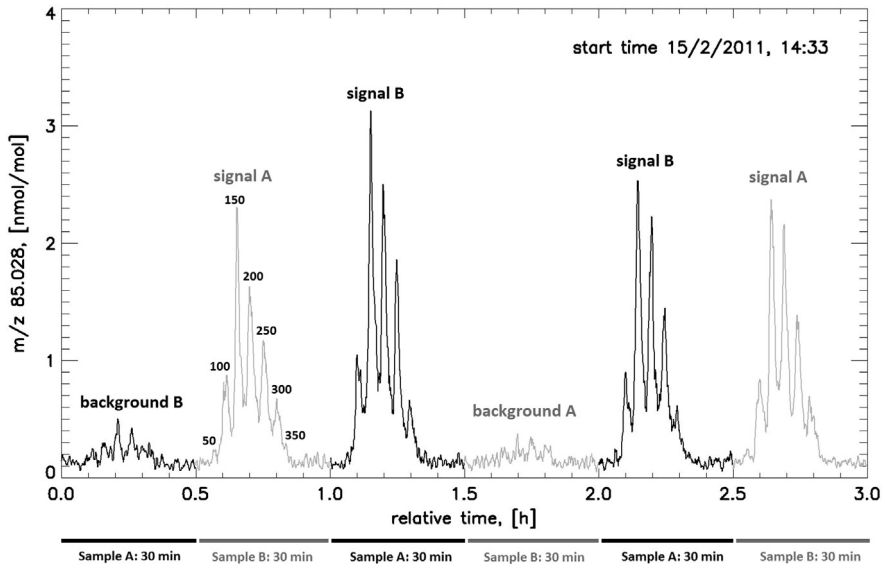

Fig. 2. The measurement cycle of the in situ TD-PTR-MS instrument; *m*/*z* 85.028 is used as an example. The time period during which sampling occurs for both inlets is indicated by the lines below the axis. The temperature steps (in degrees Celsius) are indicated in black for inlet A as an example. The aerosol signals from inlet A and B are indicated as 'signal A' and 'signal B', respectively. The background signals from inlet A and B are indicated as 'background A' and 'background B', respectively.

volatilized at the various temperature steps between 100 and 350 °C. Normally, a signal slightly above or at background level was observed at 50 °C, indicating that the collected aerosols did not significantly desorb at this temperature.

2.2.2. The offline method

2.2.2.1. Filter sampling. PM2.5 filter samples were collected on Whatman QMA quartz fiber filters using a high-volume (HiVol) filter sampler (model DHA 80) with a sampling flow of 500 L/min. The filter diameter was 15 cm, but only a part with a diameter of 14 cm was exposed to the air stream. The filters and handling equipment were carefully prepared in order to

avoid contamination. The filters were preheated at 800 °C in an oven overnight, the filter holder was cleaned with ethanol, the handling tweezers were cleaned with acetone followed by ethanol; the aluminum foil used to store the filters before and after sampling was preheated in the oven at 500 °C for 3 h. After the sampling was finished filters were brought to the laboratory and stored in the freezer at −20 °C.

During the field campaign, two one-day filters, three 2-day filters and two 3-day filters were collected. Also, two field blanks were obtained. The field blanks were treated as the regular filters but instead of being exposed to the air stream, they were kept in the filter stacks of the sampler for 3 and 6 days, respectively. The amount on the field blanks was small for most compounds compared to the amount on real samples (on average below 6%).

2.2.2.2. Thermal desorption setup in the laboratory. The oven setup for the analysis of filter aliquots consisted of a cylindrical quartz glass tube (ID=8.8 mm) surrounded by two ovens (Fig. 1B): oven 1 was 10 cm in length and oven 2 was 15 cm in length. The nitrogen flow through the oven setup was 466 mL/min (ultrapure nitrogen, 5.7 purity, Airproducts) and controlled by a thermal mass-flow controller (MKS Instruments, Germany) with a range of 500 mL/min. A filter piece of 0.39 cm^2 was placed in oven 1 using a quartz glass filter holder and the temperature of oven 1 was increased from 100 °C to 350 °C in steps of 50 °C. Every step lasted for 3 min and consisted of a ramp and dwell period of ~10 s and ~170 s, respectively. Oven 2 was used as a PTR-MS inlet extension and kept at 180 °C (which is equal to the inlet temperature of the PTR-MS) to prevent the condensation of the volatilized gasses. The organic species that evaporated at each temperature step were carried by the flow of nitrogen through the oven setup and a fraction was sampled by the PTR-MS.

2.2.3. SMPS measurements

The SMPS instrument was operated with 5 min time resolution and the particle number size distributions covering the diameter range from about 10 nm to 516 nm were measured with a log-equidistant resolution of 70 size bins in this size range. A SMPS (e.g. ten Brink et al., 1983) generally consists of a sequential set-up of an impactor, neutralizer, differential mobility analyzer (DMA) and a condensation particle counter (CPC). The operated SMPS was a modified version of a commercially available instrument (TSI 3034). The hardware and set-up of impactor, neutralizer, DMA and CPC were unchanged including the connecting parts. The software which controls the high voltage in the DMA, the correction for multiple charge, and the inversion algorithm was modified to ensure reliable measurements that are comparable to other European measurements. Additionally, the technical standards for mobility size spectrometers as recommended within ACTRIS, were followed (Wiedensohler et al., 2012).

2.3. Data treatment

Data evaluation was done with Interactive Data Language (IDL, version 7.0.0, ITT Visual Information Solutions), using custom made routines described by Holzinger et al. (2010b). The in situ TD-PTR-MS and offline data files were analyzed together, and the produced unified mass list contained m/z values of 461 ions observed during the measurements. Based on analysis of the whole dataset, nine m/z values were excluded that were associated with high instrument contamination (217.016, 218.01, 219.047, 219.173, 220.048, 221.060, 221.152, 222.057, 292.921). In addition, m/z values below 40 Da (except for m/z 31.017 and 33.033) and m/z values associated with inorganic ions (NO_2^+ and $(H_2O)_2H_3O^+$) were excluded. After these corrections the mass list contained 359 organic ions, which were considered for the evaluation presented below. Note that we allowed negative values for the mixing ratios that were sometimes obtained after background subtraction (see below).

Random and systematic uncertainties associated with the collected data were considered. Random uncertainties were calculated according to the procedure described below. Main systematic uncertainties were caused by different gas phase compounds adsorption capacity in the CTD-cell and on the quartz filters, and are approached in the main analyses. Other systematic uncertainties, caused by, e.g., distance between the in situ and offline instruments inlets and different height of the inlets, were not quantified, but their impact is believed to be minor as generally a reasonable agreement between the two datasets was observed.

2.3.1. The in situ TD-PTR-MS data

The mixing ratios of species obtained based on the in situ TD-PTR-MS data were grouped by the desorption temperature (50, 100, 150, 200, 250, 300, and 350 °C), sample type (filtered/unfiltered, i.e. background/aerosol), and inlet (A or B). The mixing ratios for each of these subsets were averaged. The dataset obtained in this way reduces the initial raw data with a 5 s time resolution to 30 min time resolution per desorption temperature per sample type per inlet matching the sampling periods on the CTD cell. Due to a problem with the heating element for the CTD cell, there were no measurements through the inlet B during the first half of in situ TD-PTR-MS measurements while filter CA10 was sampled (23 February 2011, 13:15–24 February 2011, 16:43). This was taken into account by replacing missing data with the inlet A measurements of the corresponding time period. The further in situ TD-PTR-MS data treatment was done in two different ways ((i) and (ii)):

(i) *for the comparison with offline data*: The in situ data were averaged over the time periods when filters were collected so that datasets could be directly compared. The median of the background mixing ratios over the filter sampling periods was subtracted from the average aerosol (unfiltered) signal. The mass concentration ($C_{insitu,i}$) of an observed ion 'i' signal at a

particular temperature step for a given inlet (A or B) was calculated according to Eq. (1):

$$C_{insitu,i} = \left((avg(VMR_{i,samp}) - med(VMR_{i,bgd}))M_i \times F_{inlet} \times t/S, \right. \quad (1)$$

where avg($VMR_{i,samp}$) is the average of the mixing ratios of the ion 'i' over a filter sampling period (in nmol mol^{-1} as measured in the PTR-MS), $med(VMR_{i,bgd})$ is the median of the instrument background mixing ratios of the ion 'i' over a filter sampling period (in nmol mol^{-1} as measured in the PTR-MS), M_i is the molecular weight (in g mol^{-1}) of ion 'i' (after subtraction of one a.m.u. to account for the molecular mass of the added hydrogen ion), F_{inlet} is the flow through the CTD cell during desorption in mol min^{-1}, S is the size of the air sample from which the aerosols were collected (i.e. sampled volume) in m^3, and t is the duration of a single temperature step in min. The resulting mass concentration has the unit of ng m^{-3}. Finally, the data from inlet A and B were averaged for every ion. As will be shown below, the highest artifacts appeared at the temperature level of 100 °C. Therefore, the in situ data were split into two groups based on temperature: group T100 contains organics desorbing at 100 °C and group T150–350 contains organics desorbing at 150, 200, 250, 300 and 350 °C. For data presented in Sections 3.2.1 and 3.2.3 we used m/z bins (bin size 20 Da) and averaged the m/z values of ions within the respective bins. The mass concentrations corresponding to a given m/z bin were the sum of the concentrations of all ions present in the respective mass range.

The uncertainties were up to 20% for the flow through the CTD cell, 4% for the size of a sample and typically less than 10% for the mixing ratios (mostly attributed to counting statistics and the uncertainty in the residence time in the drift tube). Note that the uncertainty in the mixing ratio does not include the uncertainty in the reaction rate constant for proton transfer, which is typically in the range $1–5 \times 10^{-9}$ cm^3 s^{-1} molecule^{-1} (Zhao and Zhang, 2004) and can thus deviate significantly from the default value (3×10^{-9} cm^3 s^{-1} molecule^{-1}) that we used here. However, assuming that the uncertainties in the reaction rate constants at a particular m/z value are the same for both methods and cancel out, the total uncertainty (ΔC_i) is calculated by means of standard error propagation to be ~22%.

(ii) *For the in situ TD-PTR-MS and SMPS data comparison*: Total OA mass concentrations (OA_{tot}) for a given time period based on the inlets A and B data and all temperature steps was calculated according to Eq. (2). In short, in situ TD-PTR-MS mixing ratios of all considered ions were multiplied by the respective molecular masses and the obtained values were summed up for all considered ions (359 ions). From this the background was subtracted obtained as a sum of the median of the background mixing ratios over a filter sampling period multiplied by the respective molecular masses. The resulting value was multiplied by F_{inlet}*t/S, which resulted in total OA mass concentrations OA_{tot} (in ng m^{-3}).

$$OA_{tot} = \left(\sum_{i=all\_ions}\sum_{j=all\_Ts}(VMR_{i,j,samp}M_i) - \sum_{i=all\_ions}\sum_{j=all\_Ts}med(VMR_{i,j,bgd})M_i\right)F_{inlet} \times t/S, \quad (2)$$

where $VMR_{i,j,samp}$ is the mixing ratio (in nmol mol^{-1}) of an ion '*i*' at a given time and given temperature, $med(VMR_{i,j,bgd})$ is the median of the background mixing ratios of an ion '*i*' over a filter sampling period for a given temperature (in nmol mol^{-1}) and M_i is the molecular weight (in g mol^{-1}) of the ion '*i*' (minus one a.m.u.); the rest of the parameters are the same as in Eq. (1). The resulting total uncertainty of OA_{tot} is calculated by means of standard error propagation to be ~20%.

2.3.2. The offline TD-PTR-MS data

Fig. 3 illustrates offline measurements and data treatment for a filter sample and a field blank (m/z 85.028 is used as an example). Similarly to the in situ TD-PTR-MS data treatment, mixing ratios obtained with a 5 s time resolution in the offline measurements were averaged over time for every temperature step. Next, the first 1.25 min of the measurements in the oven (before the temperature ramp was started) was averaged for every considered ion and used as instrument background and directly subtracted from the ion signal intensities obtained at other temperature steps. This procedure was applied to both normal filter samples and field blanks. In total, 5 field blank measurements were used: 3 replicas for CA3 and 2 replicas for CA14, all replica measurements were treated equally. The mixing ratio of the ion '*i*' for the field blank ($VMR_{i,fb}$) was calculated as a median of the mixing ratios of all field blank measurements at each temperature step.

For the filter samples, we used Eq. (3) to obtain mixing ratio of the ion '*i*' (VMR_i), corrected for the field blank and instrument background:

$$VMR_i = VMR_{i,0} - VMR_{i,instrbgd} - (VMR_{i,fb} - VMR_{i,instrbgd\_fb}), \quad (3)$$

where $VMR_{i,0}$ is the uncorrected mixing ratio of the ion '*i*', and $VMR_{i,fb}$ is the mixing ratio of the ion '*i*' on the field blank, $VMR_{i,instrbgd}$ and $VMR_{i,instrbgd\_fb}$ – are the respective background mixing ratios during sample and field blank measurements, all in nmol mol^{-1}.

After the field blank and background subtraction, the resulting mixing ratio VMR_i (nmol mol^{-1}) was converted to the mass concentration $C_{off,i}$ in ng m^{-3} as follows:

$$C_{off,\ i} = \frac{VMR_i * M_i * V_{nitrogen}}{V_{samp} * f}, \quad (4)$$

where VMR_i is the mixing ratio obtained in Eq. (3) and M_i is the molecular weight of the ion '*i*' (minus one a.m.u.), $V_{nitrogen}$ is the volume of nitrogen used for desorption at a single temperature step in mol, V_{samp} is the sampled air volume in m^3, f is the area of the measured filter aliquot divided by the area of the whole filter (fraction of the filter). The resulting mass concentration has the unit of ng m^{-3}. All steps mentioned above were done separately for every temperature level and

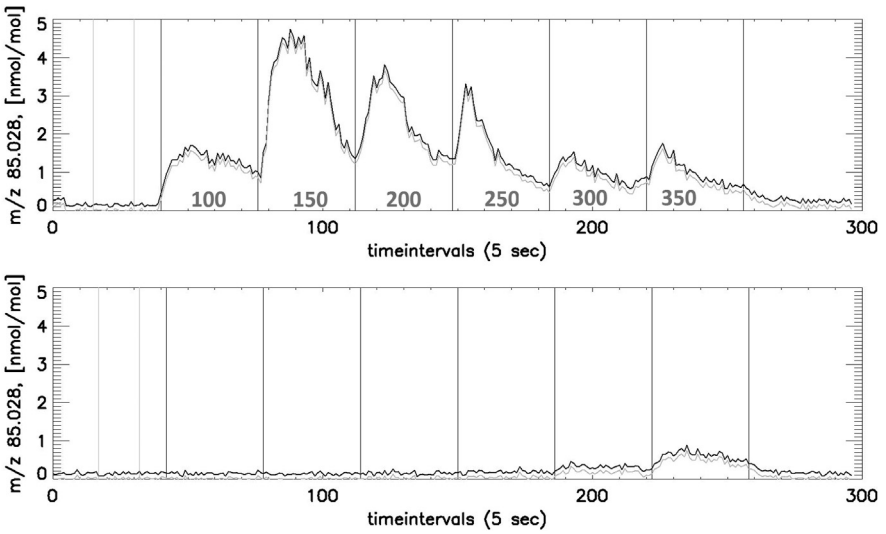

Fig. 3. Example of an offline measurement of m/z 85.028 of the filter CA12 (upper chart) and the field blank CA3 (lower chart). The black line is the original time series and gray line is the time series obtained after subtraction of the instrument background (i.e. the mean signal between the first two vertical lines plotted in red). The vertical black lines indicate the integration borders of the temperature steps. The temperature steps (in degrees Celsius) are indicated in gray for the upper chart as an example.

every organic ion, and then the resulted mass concentrations were grouped into group T100 (data obtained at 100 °C) and group T150–350 (data obtained at 150, 200, 250, 300 and 350 °C) to match the in situ TD-PTR-MS data.

The uncertainties in $VMR_{i,0}$ were calculated by propagating the uncertainties in measured mixing ratios on individual filter replicas (10%) to the average mixing ratio over all filter replicas, which resulted in 6% uncertainty. As above, the uncertainties in the mixing ratios due to the uncertainty in reaction rate constant were not considered (see Section 2.3.1). The uncertainties in the other mixing ratios ($VMR_{i,instrbgd}$, $VMR_{i,fb}$ and $VMR_{i,instrbgd\_fb}$) were neglected as for the most significant ions (comprising on average 80% of the total mass) the signal was higher than the background plus two standard deviations. Therefore, the uncertainties in VMR_i were assumed to be equal to the uncertainties in $VMR_{i,0}$ (6%). The uncertainties were up to 0.7% for the volume of nitrogen, 2% for the sampled volume, 5% for aliquot fraction. This resulted in the maximum total uncertainty of ~8% for the mass concentration of individual ions ($\Delta C_{off,i}$) calculated by means of error propagation.

2.3.3. The SMPS data

The raw SMPS data had a time resolution of 5 min and were averaged to match the sampling time of the TD-PTR-MS. In order to transform initial particle size-binned SMPS data (in number of particles per a size bin) into mass concentration B (in ng m^{-3}) Eq. (5) was used.

$$B = \frac{4}{3}\pi * \left(\frac{D_p}{2}\right)^3 * n_N(D_p) * \rho, \tag{5}$$

where D_p is the bin-central diameter (in μm) and $n_N(D_p)$ is the number of particles per cm^{-3} that have diameter between D_p and $D_p + dD_p$, ρ is the average particle density in g cm^{-3}, 1.5. The obtained SMPS aerosol mass concentrations in ng m^{-3} were used to be compared with the in situ TD-PTR-MS mass concentrations.

2.3.4. Evaluation of ion weight and chemical composition

In order to perform the analysis based on different classes of chemical compounds, the masses from the mass list were associated with molecular formulas based on the mass library (Holzinger et al., 2010b, 2013). The library contains species with up to 8 atoms of oxygen and up to 2 atoms of nitrogen. Hydrocarbons, species containing 1, 2 and 3 oxygen atoms and nitrogen-containing species were grouped in the following classes of ions: HCs, O-1, O-2, O-3 and N-compounds, respectively. All other species (mostly species that could not be matched) were grouped into the class 'other compounds'. Species belonging to O-1, O-2 or O-3 class contained no nitrogen atoms. Species belonging to N-compounds class could contain oxygen atoms. Total OA mass concentrations of a particular group of ions measured during a filter sampling period k with in situ technique ($OA_{insitu,k}$) and on filters ($OA_{off,k}$) were calculated by summing up OA mass concentrations $C_{insitu,i}$ and $C_{off,i}$ of the ions in the group, respectively.

For 288 of the 359 ion masses more than one chemical formula was possible. In these cases we applied the following rules: if the mass was odd, then the advantage was given to a formula containing only carbon, oxygen and hydrogen. If no such formula could represent a considered mass, then the formula containing nitrogen was chosen. If the mass was even, then in most cases it would attribute to nitrogen- or carbon-13-containing compounds. The preliminary advantage was

given to carbon-13-containing compounds. But for this formula to be selected, the signal of the ion had to be lower than the signal of the ion with m/z-1 multiplied by the number of carbons contained in the compound and the factor 0.022. Otherwise, the formula containing nitrogen was chosen. If there were still several formulas after applying the criteria, the formula with the smallest deviation from the detected mass was chosen.

To compare the measurements of the ion classes mentioned above, the ratio of offline and in situ mass concentrations (R) was calculated as the average of $OA_{off,k}/OA_{insitu,k}$ ratio over all filter sampling periods for the chosen ion class using

$$R = \text{average}\left(\sum_{k=filters} \frac{OA_{off,k}}{OA_{insitu,k}}\right), \tag{6}$$

The uncertainty of R (ΔR) was calculated in three steps. In the first step, the uncertainties in $OA_{insitu,k}$ and $OA_{off,k}$ were calculated. The uncertainty of $OA_{insitu,k}$ ($\Delta OA_{insitu,k}$) was calculated using

$$\Delta OA_{insitu,k} = \frac{\sqrt{\sum_{i=ions} \Delta VMR_i'^2 * VMR_i'^2 + 0.042 * \left(\sum_{i=ions} VMR_i'\right)^2}}{\sum_{i=ions} VMR_i'}, \tag{7}$$

where 'ions' refers to the ions in the chosen class of compounds, VMR_i' is the OA mixing ratio of the ion 'i' averaged over a filter sampling period k with subtracted background (equal to $avg(VMR_{i,samp}) - med(VMR_{i,bgd})$ in Eq. (1)), 0.042 is a factor taking into account uncertainties in the size of a sample and the flow through the CTD cell during desorption (S and F_{inlet} in Eq. (1)). $\Delta VMR_i'$ is the uncertainty of the OA mixing ratio VMR_i' (3.4%) calculated as follows. First, the uncertainties in the mixing ratios of an individual ion ($\Delta VMR_{i,samp}$, 10%) and ($\Delta VMR_{i,bgd}$, 10%) were propagated to the average mixing ratio over a filter sampling period. Then the squared root of the sum of the resulting relative uncertainties was taken to estimate the uncertainty of VMR_i'.

The uncertainty of $OA_{off,k}$ ($\Delta OA_{off,k}$) was calculated as follows:

$$\Delta OA_{off,k} = \frac{\sqrt{\sum_{i=ions} \Delta C_{off,i}{}^2 * C_{off,i}{}^2}}{\sum_{i=ions} C_{off,i}} \tag{8}$$

where 'ions' refers to the ions in the considered class of compounds and $\Delta C_{off,i}$ is the uncertainty of $C_{off,i}$ (8%).

In the second step, the uncertainty of $r_k = OA_{off,k}/OA_{insitu,k}$ for a filter sampling period k (Δr_k) was calculated as a squared root of the sum of the squared relative uncertainties $\Delta OA_{off,k}$ and $\Delta OA_{insitu,k}$. In the third step, the uncertainty of the average ratio R was calculated using

$$\Delta R = \frac{\sqrt{\sum_{k=N} \Delta r_k{}^2 * (r_k)^2}}{\sum_{k=N} r_k}, \tag{9}$$

where N is the number of filter sampling periods considered (7).

3. Results

3.1. Comparison of the in situ TD-PTR-MS and SMPS data

In Fig. 4 we compare OA measured by the in situ TD-PTR-MS with the total aerosol mass concentrations (in ng m^{-3}) obtained from the SMPS measurements in the time period from 15 February 2011 till 5 March 2011. Overall, the organic mass detected with the TD-PTR-MS constitutes 7% of the aerosol mass detected with the SMPS. The temporal variation of organic and total aerosol mass concentration is similar, and similar clean and polluted periods can be distinguished with both instruments. The correlation coefficient between in situ TD-PTR-MS data (averaged over both inlets) and SMPS data is 0.54 (r^2), indicating that the fraction of the OA in the total aerosol is rather stable over the abovementioned time period. A higher correlation is not expected due to several reasons: (i) the significant contribution of inorganic aerosol to the SMPS signal, (ii) different sampling heights and locations and (iii) different cutoffs for two instruments (2.5 μm for the in situ TD-PTR-MS and 0.5 μm for the SMPS measurements). The correlation coefficient between mass concentrations obtained from inlet A and inlet B data is 0.89 (r^2), and the mass concentrations agree within the estimated accuracy of ±30% (Holzinger et al., 2013), indicating a reasonable qualitative and quantitative correspondence between the two inlets.

3.2. Comparison of the offline and in situ TD-PTR-MS data

The periods of filter sampling are indicated in Fig. 4. The time periods corresponding to the sampling periods of CA5, CA6, CA10, CA11, CA12, CA13 and CA15 are referred to as t5, t6, t10, t11, t12, t13 and t15, respectively. These time periods can be separated into three categories depending on the ambient air conditions: normal (t5, t6, t10), polluted (t12, t13) and mixed (t11, t15).

3.2.1. Comparison based on different m/z ranges

For the presented analysis, separation of the detected ions into the following three mass ranges has proven to be most indicative: $31 < m/z < 191$, $191 < m/z < 291$, $m/z > 291$ Da (Fig. 5). Fig. 5A and B show scatter plots of offline mass concentrations versus in situ TD-PTR-MS mass concentrations for the groups T100 and T150–350 with the 1:1 line shown for reference. For most compounds from group T100 (constituting 0.1–3% of the total OA mass measured with the in situ technique), much higher concentrations are measured by the offline method (see Fig. 5A). A poor correlation ($r^2=0.21$) between the offline and the in situ TD-PTR-MS method is observed. The ratio of the total measured OA mass on the filters to the total aerosol mass measured with the in situ TD-PTR-MS (further called 'ratio') is 10.12. Such a high ratio can be explained by the adsorption of organic gas phase compounds on the quartz fiber filters during sampling. This kind of adsorption is much reduced during the in situ TD-PTR-MS sampling, because a significantly smaller surface area is exposed to the air stream and the material onto which air is sampled is more inert. A large fraction of the adsorbed gases evaporates at the lowest desorption temperature of 100 °C. Relatively few compounds from the actual aerosol evaporate at this temperature (100 °C), as seen by the mostly low concentrations in the in situ TD-PTR-MS measurements. Only for a few m/z bins in the mass range $m/z > 291$ Da (green points, Fig. 5A) the in situ TD-PTR-MS method yields similar or even higher

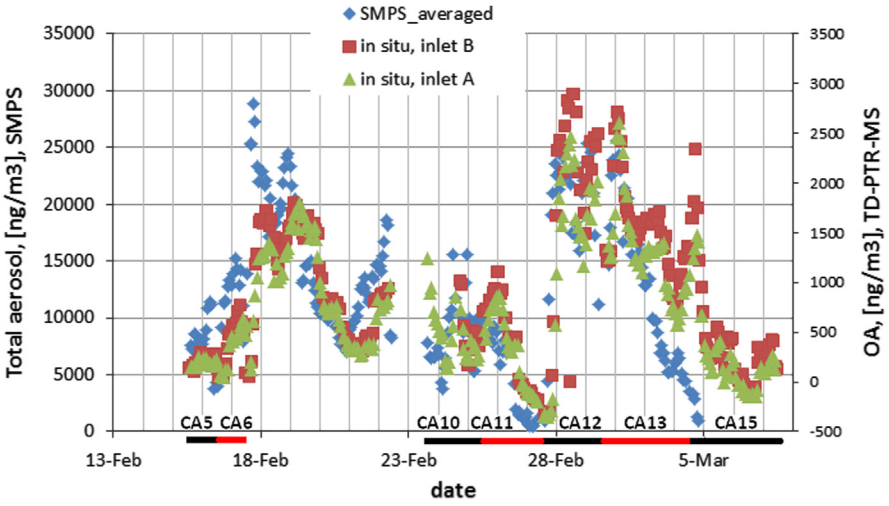

Fig. 4. Comparison of the organic aerosol mass concentrations measured with the in situ TD-PTR-MS technique (inlet A and inlet B) and total aerosol mass concentrations measured with the SMPS method (SMPS_averaged). The sampling periods for the filters are underlined below the *x*-axis with the respective filter names above.

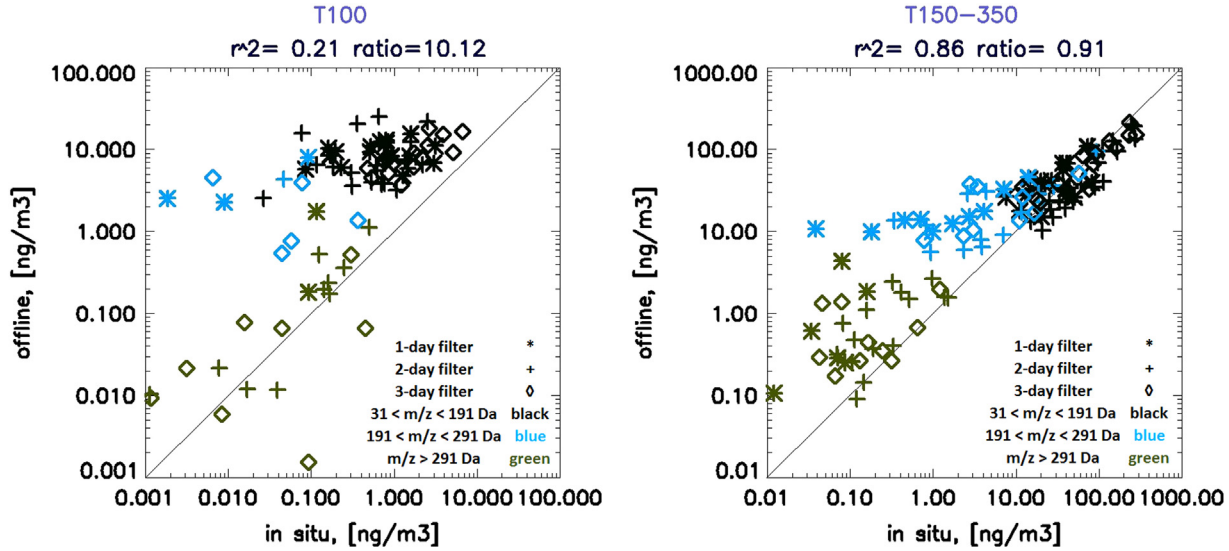

Fig. 5. Correlation plots for the offline and in situ TD-PTR-MS data (shown as 'offline' and 'in situ', respectively): (A) group T100 (compounds desorbed at 100 °C), (B) group T150–350 (compounds desorbed at 150–350 °C). Black data points correspond to m/z values in the range $31 < m/z < 191$, blue – to m/z values in the range $191 < m/z < 291$, green – to m/z values > 291 Da. Asterisks are used to indicate 1-day filters, pluses – 2-day filters, diamonds – 3-day filters.

concentrations than the offline method, but these points are mostly in the low concentration range. For the mass range $m/z > 291$ Da the ratio is 2.47, which is considerably lower than the ratio for all ions (10.12). This suggests that compounds with high molecular weight are less affected by the positive sampling artifact.

For compounds in the T150–350 group the correlation between the offline and in situ TD-PTR-MS measurements is high with $r^2 = 0.86$ and the ratio is close to unity (0.91). The ions in the mass range $31 < m/z < 191$ Da (black data points) carry the bulk of OA mass and follow closely the 1:1 line, with mass concentrations in the range of 10–300 ng m^{-3}. The concentrations of ions in the mass range $191 < m/z < 291$ Da (blue data points in Fig. 5B) are typically measured higher with the offline method. In fact, the total concentration of ions in the considered m/z bins is in the range of ~5–~100 ng m^{-3} for the offline measurements, while the in situ TD-PTR-MS data exhibit a wider range of ~0.03 to ~100 ng m^{-3}. The higher concentrations measured with the offline TD-PTR-MS are again likely caused by the contribution of adsorbed gas phase compounds to the OA signal. Ions detected in the mass range $m/z > 291$ Da (green data points in Fig. 5B) show mixed features. The concentrations of ions of several m/z bins closely follow the 1:1 line, while ions of other m/z bins exhibit higher concentrations when measured with the offline method. The data points for the ions in this mass range are poorly correlated ($r^2 = 0.01$), and the ratio of 5.23 is much larger than for all ions (0.91). The observed positive artifact for many ions in this group is attributed to adsorption of semivolatile gas phase compounds on the quartz filters, which do not fully desorb at 100 °C. Overall, the contribution of ions in the mass range $m/z > 291$ Da to the total signal is minor (less than 2% of the measured OA mass) and therefore this group of ions is not considered in the following section.

3.2.2. Bulk comparison of total OA and OA in different m/z ranges

The total OA mass concentrations for in situ TD-PTR-MS and offline measurements are calculated for the following mass ranges: all ions, $31 < m/z < 191$ Da and $191 < m/z < 291$ Da for group T150–350 (Table 2). For the group T100 we calculated only the total concentration of all ions (Table 3).

The bulk comparison also shows that the compounds detected on the filters at 100 °C are mostly due to gas phase SVOCs because for all time periods the ratios are much higher than unity (Table 3). For the CA12 filter sampled during the polluted

Table 2
Total measured aerosol concentrations (in ng m^{-3}) with the offline and in situ TD-PTR-MS techniques for group T150–350 (compounds desorbed at 150–350 °C) for three mass ranges: (a) all ions, (b) $m/z < 191$, (c) $191 < m/z < 291$. Number of days during which air was sampled on filters is indicated. Ratio (offline/in situ) and difference (offline − in situ) are shown as well.

Filter ID	CA5	CA6	**CA10**	**CA11**	**CA12**	CA13	CA15
(a) All ions							
offline (ng m^{-3})	342.4	536.1	316.4	341.1	1237.5	1112.9	371.5
in situ (ng m^{-3})	191.9	353.2	486.4	366.9	1543.6	1386.6	324.9
Ratio	1.8	1.5	0.7	0.9	0.8	0.8	1.1
Difference	150.4	182.9	−170.0	−25.8	−306.1	−273.7	46.6
(b) $31 < m/z < 191$							
Offline (ng m^{-3})	256.8	421.5	260.6	279.2	1011.4	953.7	305.1
in situ (ng m^{-3})	181.7	331.8	451.9	346.9	1392.6	1292.7	307.0
Ratio	1.4	1.3	0.6	0.8	0.7	0.7	1.0
Difference	75.0	89.7	−191.4	−67.7	−381.2	−339.0	−1.9
(c) $191 < m/z < 291$							
Offline (ng m^{-3})	76.0	106.5	50.6	55.0	219.5	154.9	61.7
in situ (ng m^{-3})	10.1	22.1	32.5	19.0	147.8	91.1	17.8
Ratio	7.5	4.8	1.6	2.9	1.5	1.7	3.5
Difference	65.9	84.4	18.2	36.0	71.8	63.8	43.9
# of sampling days	1	1	2	2	2	3	3

Table 3
Total measured aerosol concentrations (in ng m^{-3}) with the offline and in situ TD-PTR-MS techniques for the group T100 (compounds desorbed at 100 °C). Number of days during which air was sampled on filters is indicated. Ratio (offline/in situ) and difference (offline − in situ) are shown as well.

All ions							
Filter ID	CA5	CA6	CA10	CA11	CA12	CA13	CA15
Offline (ng m^{-3})	77.2	104.8	54.9	49.1	175.0	100.2	55.9
in situ (ng m^{-3})	4.1	11.2	8.6	3.9	0.9	27.0	5.4
Ratio	18.7	9.4	6.3	12.6	189.8	3.7	10.3
Difference	73.1	93.6	46.2	45.2	174.0	73.2	50.5
# Of sampling days	1	1	2	2	2	3	3

period, the ratio (189.8) is more than 10 times higher than for the other 2- and 3-day filters. This is likely caused by the polluted conditions during the t12 period and presumably high levels of SVOCs in the gas phase. On the other hand, the in situ detected OA at 100 °C is only 0.9 ng m^{-3}, which is the lowest among all time periods, potentially reflects over-correction of the background and additionally explains the high ratio (189.8). In fact, both artifacts are likely to cause this exceptional discrepancy between the in situ and the offline method at 100 °C. Overall, the total OA mass detected at 100 °C with both the in situ and the offline method represents only a rather small fraction of the OA mass detected at 150–350 °C (0.1–3% for in situ, 9–23% for offline measurements).

In Table 2 a clear difference between 1-day and 2-, 3-day filters can be seen for the group containing all ions corresponding to the compounds that desorb at 150–350 °C: the ratios are higher for 1-day filters (1.5–1.8) than for 2-, 3-day filters (0.7–1.1). It has been previously shown that positive artifacts are higher for the filters sampled during shorter time periods. Subramanian et al. (2004) found a positive offset in the measured aerosol mass concentrations of ~0.5 μg-C/m^3 for filters sampled for 24 h and an even larger offset of ~0.7 μg-C/m^3 for filters sampled for 4–6 h. The adsorption of gas phase SVOCs is likely the main process leading to such positive artifacts and in our dataset it is strongest for 1-day filters (50–80% of the total aerosol mass).The relative percentage of the positive artifacts observed here are higher than the artifacts described in the literature for 1-day quartz fiber filters (up to 30% of organic carbon mass, e.g. Subramanian et al., 2007). This might be caused by the lower absolute aerosol concentrations measured in the current study and is also reflected by absolute differences (0.2–0.3 μg/m^3, see CA5 and CA6 in Tables 2 and 3) that are at the lower end of reported ranges in the literature.

For 1-day filters the difference in the total OA mass concentrations measured with the offline and in situ techniques is similar for mass ranges $31 < m/z < 191$ Da and $191 < m/z < 291$ Da (see Table 2, 'difference'). That indicates a similar absolute contribution of gas phase SVOCs to the positive artifacts for these mass ranges for 1-day filters. However, for 2- and 3-day filters a positive artifact was observed for mass range $191 < m/z < 291$ Da (18.2–71.8 ng m^{-3}), and for the mass range $31 < m/z < 191$ Da a negative artifact prevails (-1.9 to -381.2 ng m^{-3}). With the exception of CA15, for 2- and 3-day filters the negative artifact was higher than the positive artifact. The total offline OA was therefore 7–35% lower than the in situ measurement, e.g., for the t13 time period we observe OA mass concentration 1112.9 ng m^{-3} with the offline technique and 1386.6 ng m^{-3} with the in situ technique (Table 2).

Negative artifacts may be caused by evaporation of condensed SVOCs from particles sampled on the filters as was shown for 3- and 4-ring PAHs by Coutant et al. (1988). However, Holzinger et al. (2013) showed that more volatile aerosol (semivolatile and primary OA) can be associated with ions with $m/z > 200$ Da, that is the mass range ($191 < m/z < 291$ Da) where a positive artifact prevails even for the 2- and 3-day filters. Therefore, a second process must contribute and cause the negative artifact in the mass range $31 < m/z < 191$ Da, that is the incomplete desorption of OA components from the large surface of the quartz filters during heating and possibly catalytic chemical reactions that produce other (undetectable) species. This is consistent with the findings of Holzinger et al. (2013) who showed that low volatility OA is rather desorbed by thermal decomposition than by evaporation and that undetectable products such as CO_2 and CO are produced along with detectable species with molecular weights below 200 Da. These processes are the likely cause for the observed negative artifact since they are expected to be stronger for the offline method due to the stronger affinity of aerosol compounds to the quartz fiber filter surface.

Only a very minor negative artifact was observed for CA15 sampled during mixed (mostly clean) air mass conditions, possibly indicating a compensation of positive and negative artifacts in the mass range $31 < m/z < 191$. This may be explained by the following. Presumably lower levels of condensed SVOCs are sampled and consequently there is less organic mass to evaporate. This hypothesis is supported by the fact that final sampling of CA15 filter was performed in the clean air conditions (see Fig. 4) with likely lower concentrations of SVOCs, and the fact that SVOCs on the filters are in equilibrium with sampled air (e.g., Turpin et al., 2000).

The highest absolute negative artifacts were observed for the filters CA12 and CA13 sampled during the polluted conditions (-306.1 and -273.7 ng m^{-3}, respectively). This might be caused by the higher volatility of condensed compounds sampled in the polluted conditions, causing desorption of some of these compounds during sampling on the filters. Such compounds could be hydrocarbon-like OA, which possess higher volatility than other OA (Huffman et al., 2009) and can explain the highest negative artifacts during the pollution event in case contribution of these compounds to the total measured OA is substantial.

3.2.3. *Comparison based on the chemical composition*

Due to the high mass resolution of the PTR-MS it is possible to assign empirical formulas to the measured masses and therefore determine the chemical composition. This allows to investigate in more detail the behavior of different compound classes on filters. Fig. 6 shows the ratios of offline/in situ TD-PTR-MS measurements for the considered ion classes ('other compounds', O-1, O-2, O-3, N-compounds and HCs) with error bars indicating uncertainty calculated by means of standard error propagation. Note that the ion classes are no direct projection of compound classes in OA. For example, a hydrocarbon ion can be also produced from oxygenated compounds when the oxygen group is lost in the process of thermal desorption or proton transfer ionization. For group T100 (not shown), ratios of offline/in situ TD-PTR-MS measurements for all ion classes are significantly higher than unity ($5 < \text{ratio} < 48$). The highest artifacts were observed for the following classes of compounds at 100 °C (the ratios are given in the brackets): N-compounds (48), O-3 (30), other compounds (16) and O-2 (16). In group T150–350 most classes of compounds have ratios close to unity. Only hydrocarbons and 'other compounds' have

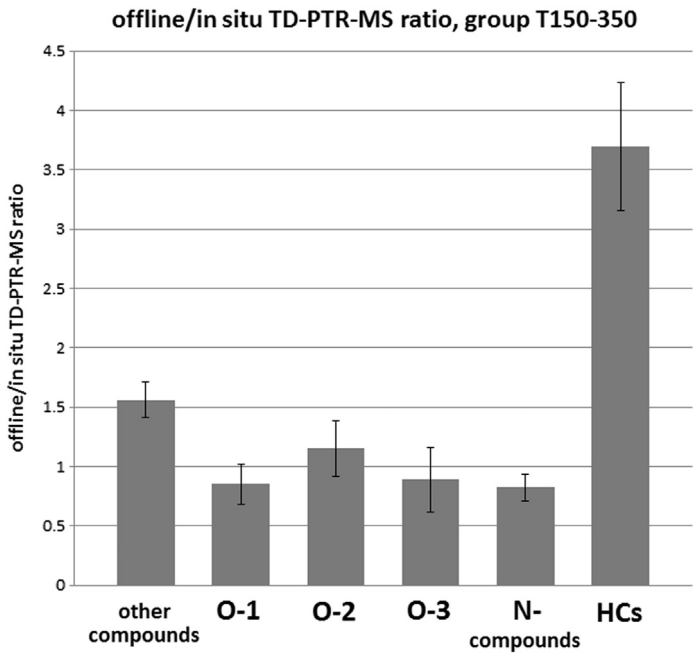

Fig. 6. Chemical speciation plot for the offline/in situ TD-PTR-MS ratios with the corresponding standard error bars for six classes of compounds in the T150–350 group: 'other compounds', O-1, O-2, O-3, N-compounds and HCs.

ratios substantially higher than unity (3.70 ± 0.54 and 1.56 ± 0.15, respectively). To understand the absolute contribution of a chemical class to artifacts, the fractions of the total OA mass (based on the in situ measurements and averaged over all filter sampling periods) for group T150–350 were calculated to be 0.15, 0.23, 0.21, 0.21, 0.16 and 0.04 for 'other compounds', O-1, O-2, O-3, N-compounds and HCs, respectively. Our results suggest that the positive artifact results to the largest part from primary emissions and not from compounds that have been heavily processed in the atmosphere. Although hydrocarbon ions may also be produced from oxygenated compounds (see above), hydrocarbon ions are nevertheless a tracer for primary emissions that have not been strongly processed in the atmosphere.

N-compounds are found to be slightly but significantly lower on filters compared to the in situ measurements (ratio $= 0.82 \pm 0.11$). This might be caused by artifacts occurring during filter sampling and/or during the thermal desorption process in the laboratory. However, losses of N-containing species during filter sampling are unlikely, since Holzinger et al. (2013) showed that nitrogen-containing compounds in the OAs are typically less volatile than other compounds. Therefore we suggest that the higher affinity of N-containing species to the surface of the quartz fiber filters causes incomplete desorption and thus the lower detected signals.

For O-1, O-2 and O-3 compounds the ratios (0.85 ± 0.17, 1.15 ± 0.23 and 0.89 ± 0.28, respectively) are not significantly different from unity indicating a good quantitative correspondence between offline and in situ measurements. This suggests that oxygen-containing compounds may contribute only to a minor extend to observed positive and negative artifacts, and that no significant charring on the filters occurs to these compounds during thermal desorption.

4. Conclusions

An offline method to study the chemical composition of organic aerosol using filter sampling followed by analysis in the laboratory using PTR-TOF-MS has been presented and compared to in situ TD-PTR-MS measurements. The high mass resolution of the PTR-TOF-MS allows a more detailed investigation of nature of the artifacts occurring during filter sampling, including chemical speciation.

At the 100 °C desorption step the offline measurements yielded much higher mass concentrations of most compounds than the in situ measurements (offline/in situ ratio is ~ 10). The likely reason for higher offline yields is adsorption of gas phase SVOCs on the large surface of the quartz filters.

Generally good correlation between offline and in situ method was observed for the desorption steps 150–350 °C (r^2 is 0.86 and offline/in situ ratio is 0.91). However, for filters sampled for 1 day (CA5, CA6) a large positive artifact has been observed (50–80% of the total aerosol mass) and also attributed to the adsorption of SVOCs on the large quartz fiber filter surface. For the filters sampled for 2 and 3 days (CA10–CA15) the agreement between offline and in situ PTR-MS measurements for total organic mass was quantitatively better than for 1-day filters. However, for most 2- and 3-day filters negative artifacts occurred. The negative artifacts were attributed to incomplete desorption of aerosols from the filters during the offline measurements and chemical reactions on the filters.

A chemical composition analysis was performed for the compounds detected at 150–350 °C. For oxygen-containing compounds the correspondence between the offline and in situ TD-PTR-MS measurements was within the levels of uncertainty. For hydrocarbon ions and ions molecular formula of which could not be identified, significantly higher concentrations were measured by the offline method (3.70 ± 0.54 and 1.56 ± 0.15, respectively). For nitrogen-containing compounds lower concentrations were measured by the offline technique, which potentially indicates a high affinity of these compounds to the quartz filter surface. However, the latter needs to be investigated further.

Acknowledgments

The TD-PTR-MS has been funded by the Netherlands Organisation for Scientific Research (NWO) under the ALW-Middelgroot program (Grant 834.08.002). We would like to acknowledge Carina van der Veen, Henk Snellen, Michel Bolder and Marcel Portanger of Utrecht University, the Netherlands for the excellent technical support. We would like to thank Mattia Monaco for the filter sampling in the field. The authors gratefully acknowledge the NOAA Air Resources Laboratory (ARL) for the provision of the HYSPLIT transport and dispersion model and/or READY website (http://www.ready.noaa.gov) used in this publication. Ulrike Dusek was funded by the Netherlands Organisation for Scientific Research (NWO, Grant 820.01.001). For the aerosol size distribution data used in this study, funding was received from the European Union Seventh Framework Programme (FP7/2007–2013) under Grant agreement no. 262254 (ACTRIS).

References

Coutant, R.W., Brown, L., Chuang, J.C., Riggin, R.M., & Lewis, R.G. (1988). Phase distribution and artifact formation in ambient air sampling for polynuclear aromatic hydrocarbons. *Atmospheric Environment*, *22*(2), 403–409.

Draxler, R.R., & Rolph, G.D. (2013). *HYSPLIT* (*Hybrid single-particle lagrangian integrated trajectory*). Model access via NOAA ARL READY Website (⟨http://www.arl.noaa.gov/HYSPLIT.php⟩). NOAA Air Resources Laboratory: College Park, MD.

Graus, M., Müller, M., & Hansel, A. (2010). High resolution PTR-TOF: quantification and formula confirmation of VOC in real time. *Journal of the American Society for Mass Spectrometry*, *21*(6), 1037–1044, http://dx.doi.org/10.1016/j.jasms.2010.02.006.

Holzinger, R., Williams, J., Herrmann, F., Lelieveld, J., Donahue, N.M., & Röckmann, T. (2010a). Aerosol analysis using a Thermal-Desorption Proton-Transfer-Reaction Mass Spectrometer (TD-PTR-MS): a new approach to study processing of organic aerosols. *Atmospheric Chemistry and Physics*, *10*, 2257–2267, http://dx.doi.org/10.5194/acp-10-2257-2010.

Holzinger, R., Kasper-Giebl, A., Staudinger, M., Schauer, G., & Röckmann, T. (2010b). Analysis of the chemical composition of organic aerosol at the Mt. Sonnblick observatory using a novel high mass resolution thermal-desorption proton-transfer-reaction mass-spectrometer (hr-TD-PTR-MS). *Atmospheric Chemistry and Physics*, *10*, 10111–10128, http://dx.doi.org/10.5194/acp-10-10111-2010.

Holzinger, R., Goldstein, A.H., Hayes, P.L., Jimenez, J.L., & Timkovsky, J. (2013). Chemical evolution of organic aerosol in Los Angeles during the CalNex 2010 study. *Atmospheric Chemistry and Physics*, *13*, 10125–10141, http://dx.doi.org/10.5194/acp-13-10125-2013.

Huffman, J.A., Docherty, K.S., Aiken, A.C., Cubison, M.J., Ulbrich, I.M., DeCarlo, P.F., Sueper, D., Jayne, J.T., Worsnop, D.R., Ziemann, P.J., & Jimenez, J.L. (2009). Chemically-resolved aerosol volatility measurements from two megacity field studies. *Atmospheric Chemistry and Physics*, *9*, 7161–7182.

Jayne, J.T., Leard, D.C., Zhang, X.F., Davidovits, P., Smith, K.A., Kolb, C.E., & Worsnop, D.R. (2000). Development of an aerosol mass spectrometer for size and composition analysis of submicron particles. *Aerosol Science and Technology*, *33*, 49–70.

Jordan, A., Haidacher, S., Hanel, G., Hartungen, E., Märk, L., Seehauser, H., Schottkowsky, R., Sulzer, P., & Mark, T.D. (2009). A high resolution and high sensitivity proton-transfer-reaction time-of-flight mass spectrometer (PTR-TOF-MS). *International Journal of Mass Spectrometry*, *286*(2–3), 122–128, http://dx.doi.org/10.1016/j.ijms.2009.07.005.

Kanakidou, M., Seinfeld, J.H., Pandis, S.N., Barnes, I., Dentener, F.J., Facchini, M.C., Van Dingenen, R., Ervens, B., Nenes, A., Nielsen, C.J., Swietlicki, E., Putaud, J. P., Balkanski, Y., Fuzzi, S., Horth, J., Moortgat, G.K., Winterhalter, R., Myhre, C.E.L., Tsigaridis, K., Vignati, E., Stephanou, E.G., & Wilson, J. (2005). Organic aerosol and global climate modelling: a review. *Atmospheric Chemistry and Physics*, *5*, 1053–1123, http://dx.doi.org/10.5194/acp-5-1053-2005.

Kirchstetter, T.W., Corrigan, C.E., & Novakov, T. (2001). Laboratory and field investigation of the adsorption of gaseous organic compounds onto quartz filters. *Atmospheric Environment*, *35*, 1663–1671.

Lambe, A.T., Chacon-Madrid, H.J., Nguyen, N.T., Weitkamp, E.A., Kreisberg, N.M., Hering, S.V., Goldstein, A.H., Donahue, N.M., & Robinson, A.L. (2010). Organic aerosol speciation: intercomparison of Thermal Desorption Aerosol GC/MS (TAG) and filter-based techniques. *Aerosol Science and Technology*, *44*, 141–151, http://dx.doi.org/10.1080/02786820903447206.

Lipsky, E.M., & Robinson, A.L. (2006). Effects of dilution on fine particle mass and partitioning of semivolatile organics in diesel exhaust and wood smoke. *Environmental Science and Technology*, *40*, 155–162.

Lopez-Hilfiker, F.D., Mohr, C., Ehn, M., Rubach, F., Kleist, E., Wildt, J., Mentel, Th. F., Lutz, A., Hallquist, M., Worsnop, D., & Thornton, J.A. (2014). A novel method for online analysis of gas and particle composition: description and evaluation of a Filter Inlet for Gases and AEROsols (FIGAERO). *Atmospheric Measurement Techniques*, *7*, 983–1001.

Mader, B.T., & Pankow, J.F. (2001). Gas/solid partitioning of semivolatile organic compounds (SOCs) to air filters. 3. An analysis of gas adsorption artifacts in measurements of atmospheric SOCs and organic carbon (OC) when using teflon membrane filters and quartz fiber filters. *Environmental Science and Technology*, *35*(17), 3422–3432.

McDow, S.R., & Hunzicker, J.J. (1990). Vapor adsorption artifact in the sampling of organic aerosol: face velocity effects. *Atmospheric Environment*, *24A*(10), 2563–2571.

Rolph, G.D. (2013). Real-time environmental applications and Display system (READY) website (⟨http://www.ready.noaa.gov⟩). NOAA Air Resources Laboratory: College Park, MD.

Schauer, C., Niessner, R., & Pöschl, U. (2003). Polycyclic aromatic hydrocarbons in urban air particulate matter: decadal and seasonal trends, chemical degradation, and sampling artifacts. *Environmental Science and Technology*, *37*, 2861–2868.

Subramanian, R., Khlystov, A.Y., Cabada, J.C., & Robinson, A.L. (2004). Positive and negative artifacts in particulate organic carbon measurements with denuded and undenuded sampler configurations. *Aerosol Science and Technology*, *38*(S1), 27–48, http://dx.doi.org/10.1080/02786820390229354.

Subramanian, R., Donahue, N.M., Bernardo-Bricker, A., Rogge, W.F., & Robinson, A.L. (2007). Insights into the primary-secondary and regional-local contributions to organic aerosol and PM2.5 mass in Pittsburgh, Pennsylvania. *Atmospheric Environment*, *41*, 7414–7433.

ten Brink, H.M., Plomp, A., Spoelstra, H., & van de Vate, J.F. (1983). A high-resolution electrical mobility aerosol spectrometer (MAS). *Journal of Aerosol Science*, *14*, 589–597, http://dx.doi.org/10.1016/0021-8502(83)90064-2.

ten Brink, H., Maenhaut, W., Hitzenberger, R., Gnauk, T., Spindler, G., Even, A., Chi, X., Bauer, H., Puxbaum, H., Putaud, J.-P., Tursic, J., & Berner, A. (2004). INTERCOMP2000: the comparability of methods in use in Europe for measuring the carbon content of aerosol. *Atmospheric Environment*, *38*, 6507–6519, http://dx.doi.org/10.1016/j.atmosenv.2004.08.027.

Turpin, J., Huntzicker, J.J., & Hering, S.V. (1994). Investigation of organic aerosol sampling in the Los Angeles basin. *Atmospheric Environment*, *28*(19), 3061–3071.

Turpin, B.J., Saxena, P., & Andrews, E. (2000). Measuring and simulating particulate organics in the atmosphere: problems and prospects. *Atmospheric Environment*, *34*(18), 2983–3013, http://dx.doi.org/10.1016/S1352-2310(99)00501-4.

Viana, M., Chi, X., Maenhaut, W., Cafmeyer, J., Querol, X., Alastuey, A., Mikuška, P., & Večeřa, Z. (2006). Influence of sampling artefacts on measured PM, OC, and EC levels in carbonaceous aerosols in an urban area. *Aerosol Science and Technology*, *40*, 107–117, http://dx.doi.org/10.1080/02786820500484388.

Viana, M., Maenhaut, W., ten Brink, H.M., Chi, X., Weijers, E., Querol, X., Alastuey, A., Mikuška, P., & Večeřa, Z. (2007). Comparative analysis of organic and elemental carbon concentrations in carbonaceous aerosols in three European cities. *Atmospheric Environment*, *41*, 5972–5983, http://dx.doi.org/10.1016/j.atmosenv.2007.03.035.

Watson, J.G., Chow, J.C., Chen, L.-W.A., & Frank, N.H. (2009). Methods to assess carbonaceous aerosol sampling artifacts for IMPROVE and other long-term networks. *Journal of the Air and Waste Management Association*, *59*, 898–911, http://dx.doi.org/10.3155/1047-3289.59.8.898.

Weber, R.J., Orsini, D., Daun, Y., Lee, Y.-N., Klotz, P.J., & Brechtel, F. (2001). A Particle-into-Liquid Collector for Rapid Measurement of Aerosol Bulk Chemical Composition. *Aerosol Science and Technology*, *35*, 718–727, http://dx.doi.org/10.1080/02786820152546761.

Wiedensohler, A., Birmili, W., Nowak, A., Sonntag, A., Weinhold, K., Merkel, M., Wehner, B., Tuch, T., Pfeifer, S., Fiebig, M., Fjäraa, A.M., Asmi, E., Sellegri, K., Depuy, R., Venzac, H., Villani, P., Laj, P., Aalto, P., Ogren, J.A., Swietlicki, E., Williams, P., Roldin, P., Quincey, P., Hüglin, C., Fierz-Schmidhauser, R., Gysel, M., Weingartner, E., Riccobono, F., Santos, S., Grüning, C., Faloon, K., Beddows, D., Harrison, R., Monahan, C., Jennings, S.G., O'Dowd, C.D., Marinoni, A., Horn, H.-G., Keck, L., Jiang, J., Scheckman, J., McMurry, P.H., Deng, Z., Zhao, C.S., Moerman, M., Henzing, B., de Leeuw, G., Löschau, G., & Bastian, S. (2012). Mobility particle size spectrometers: harmonization of technical standards and data structure to facilitate high quality long-term observations of atmospheric particle number size distributions. *Atmospheric Measurement Techniques*, *5*, 657–685, http://dx.doi.org/10.5194/amt-5-657-2012.

Williams, B.J., Goldstein, A.H., Kreisberg, N.M., & Hering, S.V. (2006). An in situ instrument for speciated organic composition of atmospheric aerosols: Thermal Desorption Aerosol GC/MS-FID (TAG). *Aerosol Science and Technology*, *40*, 627–638, http://dx.doi.org/10.1080/02786820600754631.

Yatavelli, R.L.N., & Thornton, J.A. (2010). Particulate organic matter detection using a Micro-Orifice Volatilization Impactor Coupled to a Chemical Ionization Mass Spectrometer (MOVI-CIMS). *Aerosol Science and Technology*, *44*, 61–74, http://dx.doi.org/10.1080/02786820903380233.

Zhao, J., & Zhang, R.Y. (2004). Proton transfer reaction rate constantsbetween hydronium ion (H_3O^+) and volatile organic compounds. *Atmospheric Environment*, *38*, 2177–2185.